BIOCHEMISTRY
including biophysical chemistry & molecular biology

ARTICLE

pubs.acs.org/biochemistry

Green-Fluorescent Protein from the Bioluminescent Jellyfish *Clytia gregaria* Is an Obligate Dimer and Does Not Form a Stable Complex with the Ca^{2+}-Discharged Photoprotein Clytin

Natalia P. Malikova,[†] Nina V. Visser,[‡,∥] Arie van Hoek,[‡,∥] Victor V. Skakun,[⊥] Eugene S. Vysotski,[†] John Lee,[*,@] and Antonie J. W. G. Visser[∥,§]

[†]Photobiology Laboratory, Institute of Biophysics, Russian Academy of Sciences, Siberian Branch, 660036 Krasnoyarsk, Russia

[‡]Laboratory of Biophysics, [§]Laboratory of Biochemistry, and [∥]Microspectroscopy Centre, Wageningen University, 6703 HA Wageningen, The Netherlands

[⊥]Department of Systems Analysis, Belarusian State University, Minsk 220050, Belarus

[@]Department of Biochemistry and Molecular Biology, University of Georgia, Athens, Georgia 30602, United States

ABSTRACT: Green-fluorescent protein (GFP) is the origin of the green bioluminescence color exhibited by several marine hydrozoans and anthozoans. The mechanism is believed to be Förster resonance energy transfer (FRET) within a luciferase−GFP or photoprotein−GFP complex. As the effect is found in vitro at micromolar concentrations, for FRET to occur this complex must have an affinity in the micromolar range. We present here a fluorescence dynamics investigation of the recombinant bioluminescence proteins from the jellyfish *Clytia gregaria*, the photoprotein clytin in its Ca^{2+}-discharged form that is highly fluorescent (λ_{max} = 506 nm) and its GFP (*cgre*GFP; λ_{max} = 500 nm). Ca^{2+}-discharged clytin shows a predominant fluorescence lifetime of 5.7 ns, which is assigned to the final emitting state of the bioluminescence reaction product, coelenteramide anion, and a fluorescence anisotropy decay or rotational correlation time of 12 ns (20 °C), consistent with tight binding and rotation with the whole protein. A 34 ns correlation time combined with a translational diffusion constant and molecular brightness from fluorescence fluctuation spectroscopy all confirm that *cgre*GFP is an obligate dimer down to nanomolar concentrations. Within the dimer, the two chromophores have a coupled excited-state transition yielding fluorescence depolarization via FRET with a transfer correlation time of 0.5 ns. The 34 ns time of *cgre*GFP showed no change upon addition of a 1000-fold excess of Ca^{2+}-discharged clytin, indicating no stable complexation below 0.2 mM. It is proposed that any bioluminescence FRET complex with micromolar affinity must be one formed transiently by the *cgre*GFP dimer with a short-lived (millisecond) intermediate in the clytin reaction pathway.

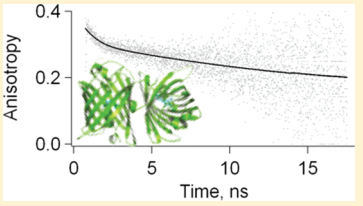

The Protein Data Bank holds more than 200 entries for green-fluorescent protein (GFP). The GFPs make up a structurally homologous protein family first discovered and isolated from some marine bioluminescent coelenterates[1] and more recently from nonbioluminescent reef organisms, mostly corals, sea anemones, and others.[2] The GFPs from the bioluminescent organisms all have a strong green fluorescence, whereas those from nonluminescent animals range in color from green to red with fluorescence efficiencies ranging from near zero to strong. Despite a very high degree of structural homology between all these fluorescent proteins, the identities of their amino acid sequences are very weak.

Most of the 200 entries are constructs derived from the natural variants for the purpose of investigating the chemistry of formation of the fluorophore or the mechanism of spectral tuning through structural perturbations of the fluorophore environment. However, the number of these more fundamental studies has been minuscule compared to a "tsunami" of reports on applications of GFP in biological and biomedical research, as well as commercial applications. Recombinant GFPs have a remarkable property in that in the process of folding, the fluorophore is formed spontaneously by an oxidative cyclization of three amino acid residues in the primary sequence.[3] Thus, it is advantageous for applications that there be no requirement for extracellular addition of a fluorescent ligand.

The GFPs were first detected and considered as participants in the bioluminescence systems of some marine organisms, first in a 1962 report of the presence of a "green protein" in extracts of the jellyfish *Aequorea victoria*[4] and later in more conclusive investigations, shown to be involved in the bioluminescence of the sea pansy *Renilla reniformis*[5] and some others, such as the hydroid *Obelia*[6] and the one subject of this work, the jellyfish *Clytia gregaria* (syn. *Phialidium gregarium*).[1,7] A 21 kDa protein purified from extracts of *A. victoria* and therefore named "aequorin" produced a blue bioluminescence color upon addition of Ca^{2+}.[1] Obelin and clytin are related proteins purified from the hydroid *Obelia* and from the jellyfish *Clytia*, respectively. These so-called Ca^{2+}-regulated photoproteins form a structural subfamily of

Received: October 17, 2010
Revised: March 20, 2011
Published: March 22, 2011

the calcium protein superfamily. The Ca^{2+}-triggered blue bioluminescence has a broad spectral distribution with a maximum in the range of 465−495 nm, depending on the type of photoprotein.[8] Because this blue bioluminescence from aequorin and the others did not match the green bioluminescence from the animal, it was proposed that GFP in some way was able to convert the bioluminescence color to its own fluorescence.[5] Unlike coelenterates, the majority of marine bioluminescent organisms emit in the blue spectral region. Convincing arguments for the survival advantage of the bioluminescence phenotype, signaling, deterrence of predators, etc., have been advanced, and for the blue color because this is optimal for transmission and reception in ocean environments.[9] There are still no good guesses about the advantage of green bioluminescence as well as the biological function of the fluorescent proteins, in nonbioluminescent organisms.

It is generally believed that the GFP acts as an acceptor in a process of Förster resonance energy transfer (FRET),[5] in which the photoprotein bioluminescence excited (S_1) state couples to the GFP's fluorophore ground state (S_0) within a protein−protein complex. According to the FRET equation, several conditions must be met for the process to be efficient: substantial spectral overlap between the bioluminescence and the absorption spectrum of GFP, a strong fluorescence of the donor, orientation of the transition dipoles of the donor and acceptor, and a separation of usually less than 50 Å. In solution studies with the purified proteins, GFP is found to cause a bioluminescence shift from blue to green at only micromolar concentrations, meaning that, at the instant of bioluminescence excitation the donor−GFP separation must be constrained within a protein−protein complex of the pair because at these low concentrations in free solution the proteins are far apart (>1000 Å). A just-published weak clytin−*cgre*GFP complex does not qualify as its K_d is in the millimolar range.[10] A protein−protein complex has also been shown to form in the case of Renilla luciferase and its conjugate GFP by the Hummel−Dreyer method of equilibrium gel filtration,[11] but attempts to produce similar results for photoprotein systems have failed or been unconvincing.[12,13]

Although many bioluminescent hydrozoans (*Aequorea*, *Obelia*, *Mitrocoma*, and *Clytia*) and anthozoans (*Renilla*, *Ptilosarcus*, and *Cavernularia*) contain GFPs,[9] actually only GFP from *Aequorea* and its numerous mutants are well-characterized, probably because the cDNA encoding GFP from *Aequorea* was cloned first almost 20 years ago.[14] Recently, cDNA for the GFP from *C. gregaria* has also been cloned, expressed in *Escherichia coli* cells, purified, and characterized.[12] In fact, this recombinant (*cgre*GFP) is only the second originating from bioluminescent Hydrozoa. Despite the fact that the GFPs from *Aequorea* and *Clytia* derive from jellyfish both belonging to Hydrozoa, the level of identity of their amino acid sequences is only 42%. However, their overall crystal structures display a very high degree of homology, which is characteristic for this family of bioluminescent proteins.[10] Other differences are that in solution, Aequorea GFP (*av*GFP) is monomeric whereas *cgre*GFP and almost all other GFPs are dimeric or form higher-order aggregates. Although their green fluorescence spectra are similar, *av*GFP has a major absorbance peak at 395 nm and a minor one at 475 nm, whereas for *cgre*GFP and Renilla GFP, for example, there is only one peak in this region at 485 nm.[3] A puzzling observation and one quite relevant to this study is the fact that in the in vitro reaction, the bioluminescence emission is shifted to the green for clytin or Renilla luciferase with only micromolar concentrations of their respective GFPs, but for aequorin, almost 100 times larger amounts are needed.[11]

In this work, we use dynamic fluorescence methods to characterize the spectral properties of Ca^{2+}-discharged clytin and its cognate antenna protein, *cgre*GFP. Clytin itself is hardly fluorescent, but the reaction product Ca^{2+}-discharged clytin could be an efficient excitation donor because it has strong fluorescence with a high degree of spectral overlap with the *cgre*GFP absorption ($S_0 \rightarrow S_1$). These fluorescence methods have been successfully employed to establish the FRET mechanism in the otherwise unrelated bioluminescence system of bacterial luciferase and its antenna protein called "lumazine protein".[15,16] Similarly, both Ca^{2+}-discharged clytin and *cgre*GFP proteins contain tightly associated fluorophores with suitable fluorescence lifetimes for anisotropy decay measurement.

We are unable to detect any stable complex of the Ca^{2+}-discharged clytin with *cgre*GFP, the same as found for clytin prior to addition of Ca^{2+}.[10] We propose, therefore, that the bioluminescence FRET complex must be one formed with a short-lived intermediate in the clytin bioluminescence pathway.

MATERIALS AND METHODS

The recombinant apo-clytin was purified from inclusion bodies and charged with coelenterazine, as previously reported for recombinant obelin.[17,18] To prepare the Ca^{2+}-discharged clytin, a concentrated solution of clytin was diluted 10-fold with 20 mM Tris-HCl (pH 7.0) containing $CaCl_2$ at a final concentration of 1 mM and then again concentrated. This procedure was repeated twice.

To produce *cgre*GFP, *E. coli* XL1-Blue cells carrying the plasmid with *cgre*GFP (GenBank accession number GU721039)[12] were cultivated at 37 °C until the culture reached an OD_{600} of 1.0. Then to induce the synthesis, 1 mM IPTG was added and the cultivation was continued overnight at room temperature to improve the maturation of *cgre*GFP. The next day the flask containing the liquid culture was refrigerated at 4 °C and kept there for 2 days to provide the maximum yield of mature *cgre*GFP.

The *cgre*GFP was purified from the supernatant on a Talon Metal Affinity Resin column (BD Biosciences) according to the manufacturer's protocol. After all the washing procedures had been conducted, the resin was suspended in 20 mM Tris-HCl (pH 7.2) and incubated under shaking with human enteropeptidase[19] at 18 °C overnight to remove the His_{10} tag. The resin was separated by centrifugation. Enteropeptidase was captured from the *cgre*GFP solution by binding with STI-Agarose containing protease inhibitor followed by precipitation of the complexes. Both recombinant proteins were of high purity according to sodium dodecyl sulfate−polyacrylamide gel electrophoresis. For the fluorescence measurements, *cgre*GFP was moved into a buffer of 20 mM Tris-HCl (pH 7.0) with 1 mM $CaCl_2$.

Time-resolved fluorescence measurements (20 °C) were taken using a mode-locked laser pumped with a continuous wave laser for excitation and time-correlated single-photon counting (TCSPC) as the detection technique, as extensively described previously.[20,21] The samples were excited with plane-polarized light pulses (0.2 ps full width at half-maximum) at an excitation frequency of 3.8 MHz, and both parallel and perpendicular polarized fluorescence intensities were detected. The time-resolved polarized fluorescence experiments on the Ca^{2+}-discharged photoprotein were performed by using 370 nm excitation and fluorescence detection with a combination of an

appropriate cutoff and interference filters peaked at 410, 466, 498, 512 and 557 nm (all filters are from Schott, Mainz, Germany). Experiments with *cgre*GFP and enhanced GFP from *A. victoria* (abbreviated as EGFP) were conducted at 470 nm excitation and fluorescence detection via the combination of 515 nm cutoff and 512 nm interference filters. In experiments with 370 nm excitation and detection at 410, 466, 498, and 512 nm, the dynamic instrumental response function of the setup was obtained by using a solution of xanthione in ethanol as a reference compound having an ultrashort fluorescence lifetime of 14 ps. The reference compound for time-resolved fluorescence decay experiments with 370 nm excitation and 557 nm detection, and 470 nm excitation and 512 nm detection, was erythrosine B in an aqueous solution having a fluorescence lifetime of 85 ps. In all experiments, the binning time was 5 ps and 4096 time channels were used. Global analysis of total fluorescence decays and fluorescence anisotropy decays using multiexponential model functions was conducted as described previously.[20,21] When not explicitly mentioned, the standard errors of the parameters were obtained from the fitting routine.

Fluorescence fluctuation spectroscopy (FFS) measurements (20 °C) were performed on the ConfoCor 2-LSM 510 combination setup (Carl Zeiss, Jena, Germany) detailed in refs 22 and 23. EGFP and *cgre*GFP were excited with the 488 nm line from an argon ion laser (excitation intensity in the range of 10−40 μW) focused into the sample with a water immersion C-Apochromat 40× objective lens N.A. 1.2 (Carl Zeiss). After passing through the main beam splitters (HFT 488/633), the fluorescence was filtered with a 505−550 nm band-pass. The pinhole for confocal detection was set at 70 μm. The microscope was controlled with Zeiss AIM version 3.2. Raw intensity fluctuation data consisting of up to 10^6 photons were collected from single measurements. The data collection time ranged between 30 and 120 s. In fluorescence correlation spectroscopy (FCS) and photon counting histogram (PCH) analysis, the same experimental fluorescence intensity fluctuations are used, but each analytical method focuses on a different property of the signal. The autocorrelation function (ACF) is the time-dependent decay of the correlation of fluorescence fluctuations and is obtained in FCS measurements yielding, for instance, molecular diffusion coefficients. The amplitude distribution of these fluctuations is calculated by PCH, yielding the molecular brightness, i.e., the number of photons emitted by one molecule per second. Both FCS and PCH give information about the molecular concentration. Very recently, a global analysis protocol has been described that simultaneously recovers the relevant and common parameters in model functions of FCS and PCH from a single fluorescence fluctuation trace.[24] The global analysis approach has been tested with experimental fluorescence fluctuation data of EGFP and dimeric EGFP (two EGFP molecules connected by a six-amino acid linker) in aqueous buffer.[24] Molecular brightness values and diffusion constants are recovered with good precision. Aqueous solutions of EGFP and *cgre*GFP were measured directly after each other so that the results can be compared. Photon counting distributions (PCDs) are generated at two different bin times of 50 and 100 μs. Rhodamine 110 (R110) (Invitrogen, Breda, The Netherlands) in water was used for calibration measurements. Although the molecular mass of R110 (508 Da) is slightly higher than that of rhodamine 6G (479 Da), we used the absolute diffusion constant of rhodamine 6G (414 $\mu m^2\ s^{-1}$ at 25 °C or 374 $\mu m^2\ s^{-1}$ at 20 °C) to determine the diffusion constants of EGFP and *cgre*GFP.[25]

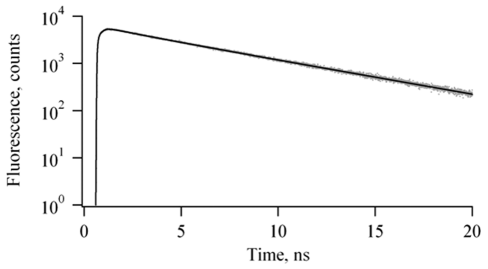

Figure 1. Single-experiment total fluorescence decay analysis of 0.2 μM calcium-discharged clytin with excitation at 370 nm and fluorescence at 512 nm. Shown are experimental (dots) and calculated (solid line) fluorescence traces. The recovered lifetime components (and percentage amplitudes in parentheses) are 48 ps (1%), 2.1 ns (11%), and 5.9 ns (88%). The quality of fit criterion $\chi^2 = 1.01$.

RESULTS

Time-Resolved Polarized Fluorescence of Ca^{2+}-Discharged Clytin. The total fluorescence decay of Ca^{2+}-discharged clytin is heterogeneous and consists of three lifetime components. An example of a single-experiment analysis taken at 512 nm detection is shown in Figure 1. We have globally analyzed the total fluorescence decay (excitation wavelength of 370 nm) at five detection wavelengths linking the three lifetimes over five experiments and keeping the amplitudes as free adjustable parameters. The obtained lifetimes are 32 ± 1 ps, 1.67 ± 0.01 ns, and 5.74 ± 0.01 ns (Table 1). Each lifetime multiplied by its normalized amplitude ($\alpha_i\tau_i$; $\Sigma\alpha_i = 1$) is the relative contribution of that lifetime component in the steady-state fluorescence intensity at that wavelength, and $\Sigma\alpha_i\tau_i$ is the first-order average lifetime. At each wavelength, the longest lifetime has by far the largest contribution and is essentially ~95% over the steady-state fluorescence spectral distribution at >466 nm (λ_{max} = 506 nm[12]).

Following the recent picosecond fluorescence spectral relaxation results for the Ca^{2+}-discharged photoproteins aequorin and obelin, the long-lifetime component of 5.74 ns can be assigned to the $S_1 \rightarrow S_0$ transition of the anion of coelenteramide, the product of the bioluminescence reaction bound to the protein.[26] This lifetime is somewhat longer than the 4 ns longest lifetime component observed for the aequorin and obelin products.[26] Fluorescence excitation of a Ca^{2+}-discharged photoprotein proceeds into the Franck−Condon state of protein-bound coelenteramide in its neutral state that, in the absence of ionization, has a fluorescence band maximum around 410 nm. Within the binding cavity of the protein, however, this primary state rapidly undergoes excited-state proton transfer (ESPT) to generate the excited coelenteramide anion. The recent picosecond relaxation study of Ca^{2+}-discharged aequorin and obelin detected a time for this ESPT to be 30 ps for the case of aequorin, and much faster for the obelin product.[26] Therefore, we assign the 32 ps time (Table 1) to the ESPT. In the relaxation study, however, several other fast processes were evident in the region of 150−500 ps, possibly arising from structural relaxation of the binding cavity. In this case of Ca^{2+}-discharged clytin, an assignment of the 1.67 ns lifetime is not obvious. Its contribution is small and only at the shorter wavelengths. Judging from the progressive, time-dependent red shift in the picosecond time-resolved emission spectra of Ca^{2+}-discharged aequorin and obelin,[26] we cannot rule out the possibility that the 1.67 ns component simply reflects this same time-dependent red shift

Table 1. Global Analysis of the Total Fluorescence Decay of Ca^{2+}-Discharged Clytin at 20 °C[a]

λ_{em} (nm)	τ_1 = 0.032 ns, $\alpha_1\tau_1$ (ns)	τ_2 = 1.67 ns, $\alpha_2\tau_2$ (ns)	τ_3 = 5.74 ns, $\alpha_3\tau_3$ (ns)	$\langle\tau\rangle = \Sigma\alpha_i\tau_i$ (ns)
410	0.026 (4%)	0.22 (34%)	0.40 (62%)	0.65
466	0.026 (3%)	0.077 (8%)	0.79 (89%)	0.90
498	0.014 (0.5%)	0.12 (4%)	2.78 (95.5%)	2.92
512	0.025 (2%)	0.030 (2%)	1.22 (96%)	1.28
557	0.008 (0.2%)	0.072 (2%)	4.12 (97.8%)	4.20

[a] Values in parentheses are the relative contributions of the lifetime component in the steady-state spectrum. Amplitudes α_i are scaled such that $\Sigma\alpha_i = 1$.

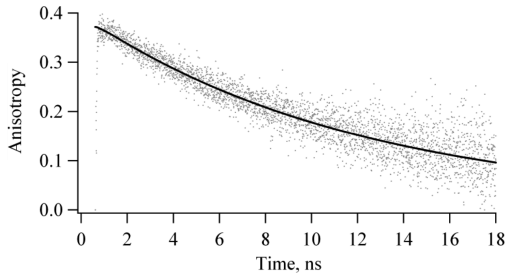

Figure 2. Single-experiment fluorescence anisotropy decay analysis of 0.2 μM calcium-discharged clytin with excitation at 370 nm and fluorescence at 512 nm. Shown are experimental (dots) and calculated (solid line) anisotropy traces. The recovered correlation time is 12.2 ns, and the initial anisotropy (at the start of the analysis) is 0.372. The quality of fit criterion χ^2 = 1.00.

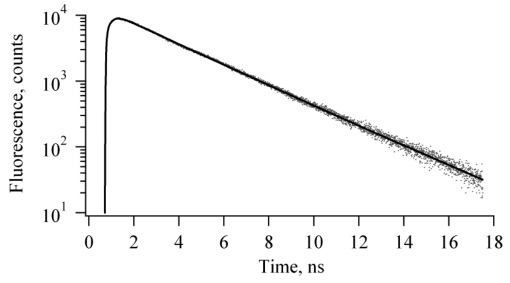

Figure 3. Single-experiment total fluorescence decay analysis of 0.57 μM *cgre*GFP with excitation at 470 nm and fluorescence at 512 nm. Shown are experimental (dots) and calculated (solid line) fluorescence traces. The recovered lifetime components (and percentage amplitudes in parentheses) are 0.86 (9%) and 2.72 ns (91%). The quality of fit criterion χ^2 = 1.20.

and is needed to obtain a good fit, and the value therefore is artifactual.

The fluorescence anisotropy decay of Ca^{2+}-discharged clytin is monoexponential with a single rotational correlation time (ϕ) of 12 ns (20 °C) characteristic of a tightly bound fluorophore rotating together with a 22 kDa protein. A typical example of single-experiment anisotropy decay analysis is given in Figure 2. We have globally analyzed three experiments taken at detection wavelengths of 498, 512, and 557 nm linking the correlation times and obtained a ϕ of 11.96 ± 0.04 ns with an initial anisotropy (extrapolated to time zero) of 0.378 ± 0.012 (average and standard error of three experiments).

Time-Resolved Polarized Fluorescence of *cgre*GFP. Single-photon timing experiments were performed using 470 nm excitation and 512 nm detection. The time-resolved fluorescence of *cgre*GFP at concentrations of <1 μM does not show a monoexponential decay. An example of a single-experiment analysis using 0.57 μM *cgre*GFP is given in Figure 3. Two lifetimes are needed to fit the decay curve, as observed previously for EGFP.[27] A predominant fluorescence lifetime of 2.78 ns and a shorter lifetime of around 1 ns with a smaller contribution are obtained. We have performed a dilution experiment starting with a concentration of 2.85 μM, followed by 0.57 μM (diluted 5-fold), 57 nM (diluted 50-fold), and 5.7 nM (diluted 500-fold), and measured the time-resolved fluorescence. The four sets of experimental data are globally analyzed linking the two lifetimes and keeping the amplitudes as freely adjustable parameters. The recovered lifetimes are 1.40 ± 0.02 and 2.780 ± 0.003 ns. All parameters are listed in Table 2. It is clear that only *cgre*GFP at the highest concentration (2.85 μM) shows monoexponential fluorescence decay with a lifetime of 2.78 ns. The more dilute samples exhibit a biexponential decay with an additional lifetime of 1.40 ns, a contribution that increases at lower concentrations.

The excited-state dynamics of *avre*GFP and EGFP have been well documented (see ref 28 for details and back references). The photophysics of both GFPs can be explained by a model of ESPT and three forms of the chromophores, a protonated A-form absorbing light at 400 nm and two deprotonated or anionic I-forms (intermediate) and B-forms absorbing at around 475 nm. The chemical structure of the A-form is the *p*-hydroxybenzylidene-imidazolinone chromophoric group. The intermediate anionic, excited form I* is supposed to be an unrelaxed form of B*. From previous excitation- and emission-resolved single-photon timing experiments with EGFP, it was established that the fluorescence decay times of the anionic I* and B* states are 3.4 and 2.7 ns, respectively.[28] In addition, the I-form is red-shifted as compared to the B-form, in both absorption and emission.

In contrast to EGFP, *cg*GFP is a natural variant of GFP but with a major increase in magnitude and red shift to 488 nm of the absorption band associated with the anionic form of the chromophore.[12] When the previous results are extrapolated to our time-resolved experiments with *cgre*GFP, the 2.78 ns lifetime can be assigned to the anionic B* state. Using excitation and emission wavelengths in our experiments, we do not find an anionic I* state for *cgre*GFP. Then what is the origin of the 1.40 ns fluorescence lifetime, which seems absent at higher protein concentrations? To explain this, we must have some background knowledge about how the single-photon timing experiments are performed. Experiments are always conducted in such a way that an emission count rate of 30 kHz is reached (in the parallel polarized channel), which is less than 1% of the laser pulse repetition rate to avoid pulse pile-up distortion. Neutral density filters regulate the energy of the excitation pulses. At high protein concentrations, a minimal amount of laser energy is needed to reach the 30 kHz count rate. However, at lower protein concentrations, the laser intensity must be gradually increased to reach this number. GFP can be easily converted photochemically

Table 2. Global Analysis of the Total Fluorescence Decay and Fluorescence Anisotropy Decay of *cgre*GFP at 20 °C

[*cgre*GFP]	τ_1 = 1.40 ns, α_1 (−)	τ_2 = 2.78 ns, α_2 (−)	$\langle\tau\rangle = \Sigma\alpha_i\tau_i$ (ns)	ϕ_T = 0.51 ns, β_1 (−)	ϕ = 34.0 ns, β_2 (−)
2.85 μM	0	1.0	2.78	0.066 ± 0.002	0.297 ± 0.001
0.57 μM	0.15	0.85	2.57	0.053 ± 0.002	0.300 ± 0.001
57 nM	0.24	0.76	2.44	0.035 ± 0.002	0.328 ± 0.001
5.7 nM	0.26	0.74	2.43	0.034 ± 0.002	0.339 ± 0.001

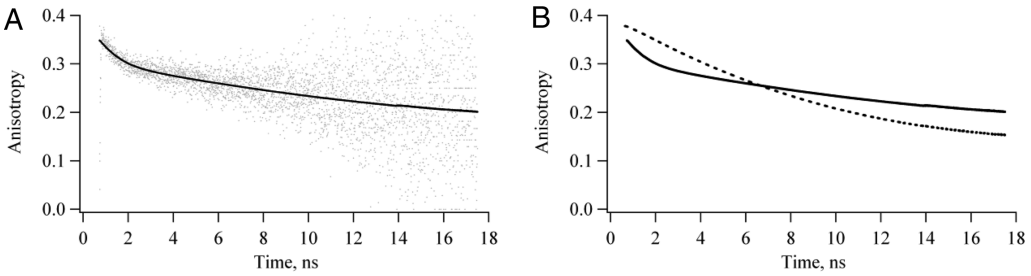

Figure 4. (A) Single-experiment fluorescence anisotropy decay analysis of 0.57 μM *cgre*GFP with excitation at 470 nm and fluorescence at 512 nm. Shown are experimental (dots) and calculated (solid line) anisotropy traces. The recovered correlation times (and amplitudes in parentheses) are 0.64 (0.049) and 34.0 ns (0.300). The quality of fit criterion χ^2 = 1.15. (B) Theoretical anisotropy traces of 0.57 μM *cgre*GFP (—) and 0.5 μM EGFP (---) (ϕ = 14 ns).

into another species.[29] Therefore, we want to surmise that the 1.40 ns lifetime is a photochemically generated other B-form. This leads to two subpopulations of the protein, B_1 (original) and B_2 (photogenerated), having two different conformations. Upon excitation with 470 nm light, two excited-state anionic forms, B_1* and B_2*, emitting independently with different lifetimes will be created.

An example of the fluorescence anisotropy decay and analysis from a single experiment is given in Figure 4A. To visually compare anisotropy decay patterns, we have coplotted the fitted anisotropy decays of EGFP (ϕ = 14 ns) and *cgre*GFP in Figure 4B. The model function to which the clearly biexponential anisotropy decay of *cgre*GFP, $r(t)$, has been fitted is

$$r(t) = [\beta_1 \exp(-t/\phi_T) + \beta_2] \exp(-t/\phi) \quad (1)$$

where ϕ_T is a short correlation time arising from reversible energy transfer between the chromophores, ϕ is the rotational correlation time of the (dimeric) protein, and β_1 and β_2 are the amplitudes. ϕ_T is the reciprocal of 2 times the transfer rate constant, k_T, where

$$\phi_T = \frac{1}{2k_T} \quad (2)$$

the factor of 2 indicates the reversibility of the FRET process. By summation and subtraction of amplitudes β_1 and β_2, information about the intra- and intermolecular transition moments can be obtained:[30]

$$\begin{aligned} \beta_2 + \beta_1 &= \frac{3}{5}\cos^2\delta - \frac{1}{5} \\ \beta_2 - \beta_1 &= \frac{3}{5}\langle\cos^2\theta_T\rangle - \frac{1}{5} \end{aligned} \quad (3)$$

where δ is the intramolecular angle between the absorption and emission transition dipole moments in one molecule and θ_T the intermolecular angle between the absorption transition dipole moment of molecule 1 and the emission transition dipole moment of molecule 2. The broken brackets in eq 3 denote an average of two values:

$$\langle\cos^2\theta_T\rangle = \frac{1}{2}(\cos^2\theta_{T1} + \cos^2\theta_{T2}) \quad (4)$$

The transition dipole moment directions in the chromophore of *av*GFP are known from polarized absorption spectra of single crystals.[31] The four sets of experimental data are globally analyzed linking the two correlation times and keeping the amplitudes as adjustable parameters. The obtained correlation times are as follows: ϕ_T = 0.51 ± 0.03 ns, and ϕ = 34.0 ± 0.5 ns. The amplitudes are listed in Table 2. The amplitude of the short correlation time (0.51 ns) depends on the *cgre*GFP concentration. The amplitude is highest (0.066) at 2.8 μM but decreases to 0.034 at 5.7 nM. The higher laser intensity used to reach a detection rate of 30 kHz emission photons at a lower concentration may induce saturation effects. At higher laser intensities, the probability of exciting two GFP fluorophores in the same dimeric protein will be enhanced. When this is the case, there will be no FRET because the coupling always takes place between one molecule in the excited state and the other in the ground state. The other remarkable observation is that at 5.7 nM, *cgre*GFP is still a 54 kDa dimer because it shows the 34.0 ns correlation time and not the 17.0 ns correlation time expected for a monomer. It must be concluded that there is very strong interaction between the protein chains.

From the fitted fluorescence anisotropy decay, we can obtain geometric information about the two fluorophores in the protein. By using eq 2 and a ϕ_T of 0.51 ns, the rate constant (k_T) equals 0.98 ns^{-1}. This rate constant can be related to the donor−acceptor separation using the Förster equation (eq 5):

$$k_T = \frac{1}{\tau_D}\left[\frac{R_0}{R}\right]^6 \quad (5)$$

where τ_D is the fluorescence lifetime of the donor (2.78 ns in this case), R is the donor−acceptor separation, and R_0 is the critical distance or Förster radius. R_0 is obtained from the well-known

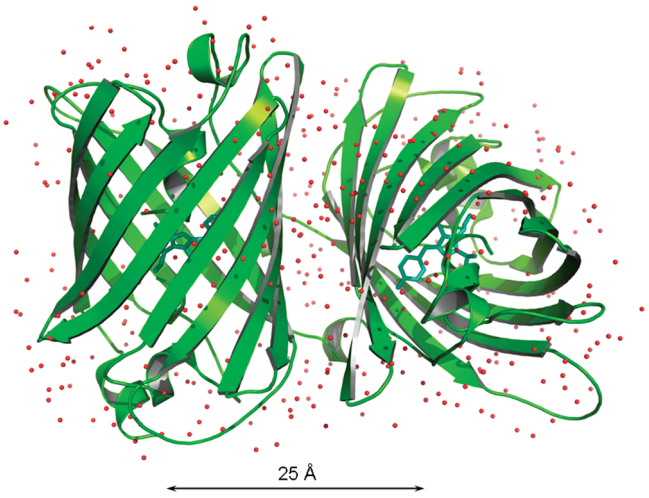

Figure 5. Structure of the *cgre*GFP dimer with its embedded water molecules (red spheres) resembling a highly concentrated aqueous solution of amino acids. It had been suggested that the appropriate value for the refractive index to be used in the FRET equation should be that for a solution of amino acids, viz., $n = 1.6$, and not that of the external solvent. This is now supported by theoretical studies. The 25 Å distance is the approximate separation of the pair of fluorophores (aqua). The structure was constructed from Protein Data Bank entry 2HPW.[10]

FRET equation that requires knowledge of the spectral overlap, the refractive index n of the intervening medium, and an orientation factor κ^2 related to the intermolecular angle between the transition moments (θ_T), which can be obtained from the difference in amplitudes (eq 3). From the amplitudes recovered from the experiment with the highest concentration, $\beta_2 - \beta_1 = 0.231$, and the result is an intermolecular angle θ_T of 32° with a κ^2 of 1.08 (the latter value was obtained from the crystal structure[10]). The original derivation of the FRET equation was for small molecule donors and acceptors freely diffusing in solution where for aqueous solution, $n = 1.33$. For FRET within a protein, however, some ambiguity about whether the applicable refractive index is of the local environment or of the bulk medium arises. Figure 5 shows that the spatial structure of the *cgre*GFP dimer with its associated waters is essentially like a highly concentrated aqueous solution of amino acids. From an analysis of the molar refraction of amino acids, it was concluded that $n = 1.6$ within a protein.[32] Recent theoretical treatments of this question conclude that, for excited-state coupling internal to a protein, $n = 1.6$,[33,34] and this results here in an R_0 of 46 Å. From eq 4, $R = 32$ Å, close to the 25 Å separation in the spatial structure that exhibits an intermolecular angle of 38° (Figure 5).

Searching for Protein Interactions between Ca^{2+}-Discharged Clytin and *cgre*GFP. We have performed time-resolved polarized fluorescence experiments with mixtures of Ca^{2+}-discharged clytin and *cgre*GFP, titrating one of the proteins into a fixed concentration of the other. The titration of a fixed concentration of 200 nM Ca^{2+}-discharged clytin with increasing concentrations of *cgre*GFP (up to 1:10 molar ratio) while monitoring the Ca^{2+}-discharged clytin fluorescence at 466 nm is not feasible because of the much stronger *cgre*GFP fluorescence leaking into the fluorescence detection channel and giving rise to an artifactual shortening of the fluorescence lifetime. The titration of a fixed concentration of 10 nM *cgre*GFP with increasing concentrations of Ca^{2+}-discharged clytin (up to 1:1000 molar ratio) while monitoring the possible increase in the rotational correlation time of *cgre*GFP is certainly feasible. It has been previously demonstrated for yellow-fluorescent protein (YFP) that correlation times of up to 50 ns can be determined.[20] A time-resolved fluorescence anisotropy experiment with the FRET-based calcium sensor Yellow Cameleon 3.60 (YC3.60, a fusion of the ECFP donor to calmodulin with a YFP variant as the acceptor) also confirms this feasibility.[21] YC3.60 without calcium bound to calmodulin possesses a flexible structure giving rise to a significantly shorter correlation time (31 ns) compared to that of the rigid calcium-bound conformation (50 ns). These experiments illustrate that a complex between Ca^{2+}-discharged clytin and *cgre*GFP having an overall rotational correlation time of 46 ns (12 ns + 34 ns) must be measurable. Apart from the fact that the additivity of masses is reflected in rotational diffusion measurements, the other advantage is that Ca^{2+}-discharged clytin does not absorb light at 470 nm, preventing spectroscopic interference.

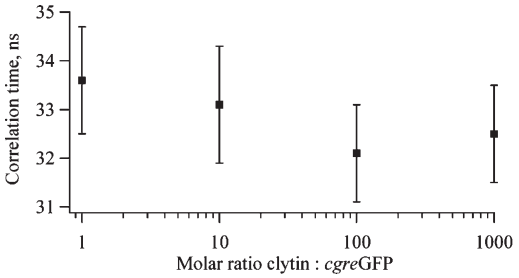

Figure 6. Titration of Ca^{2+}-discharged clytin into 10 nM *cgre*GFP by monitoring the long correlation time due to overall *cgre*GFP rotation (excitation 470 nm, detection 512 nm). The rotational correlation time of *cgre*GFP alone is 33.9 ± 1.1 ns.

The long correlation time obtained from these measurements has been plotted versus the molar ratio of *cgre*GFP to Ca^{2+}-discharged clytin in Figure 6. It is clear from these results that no increase in rotational correlation time is observed, meaning that there is no stable protein−protein complex. From these experiments, we can estimate some limiting values of any weak dissociation constant (K_d):

$$K_d = \frac{[\text{clytin}][\textit{cgre}\text{GFP}]}{[\text{clytin} - \textit{cgre}\text{GFP}]} = \frac{k_d}{k_a} \qquad (6)$$

where k_d is the dissociation rate constant (s^{-1}) and k_a the association rate constant ($M^{-1}\ s^{-1}$). Given the fixed *cgre*GFP concentration of 10 nM, the highest Ca^{2+}-discharged clytin concentration of 10 μM, and the fact that no complex was detected, any equilibrium dissociation constant must be larger than 10 μM. If we assume that ~5% of complex would escape experimental observation at the highest Ca^{2+}-discharged clytin concentration, then its K_d would have to be >0.2 mM. In agreement with these observations, Markova and co-workers[12] found no evidence of association of *cgre*GFP with either clytin or Ca^{2+}-discharged clytin, by equilibrium gel filtration. This is in contrast to the detection of a Renilla GFP−luciferase complex by the same chromatography method.[11]

Fluorescence Fluctuation Spectroscopy of EGFP and *cgre*GFP. In fluorescence correlation spectroscopy, dynamic molecular processes in the micro- to millisecond time range can be observed as fluorescent molecules at low concentrations diffuse in and out of the focus of a laser beam. To increase the signal:noise ratio, many single-molecule events are measured and

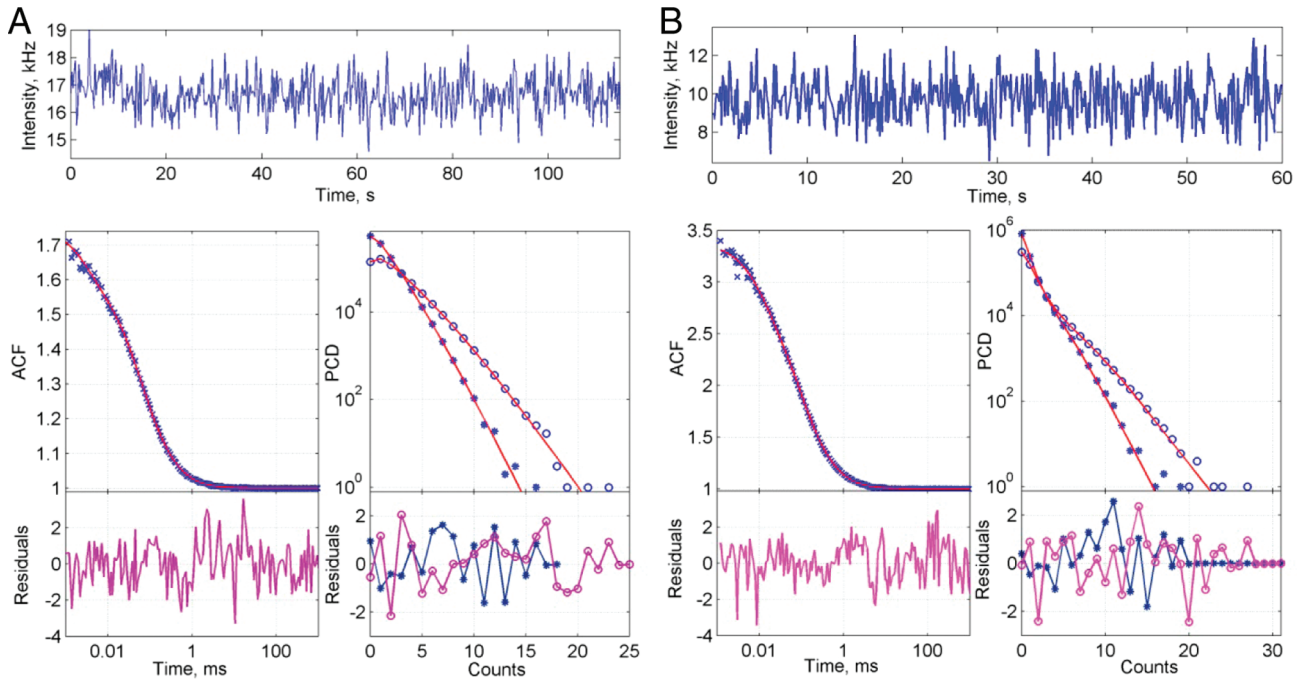

Figure 7. Results of global analysis of the autocorrelation function (ACF) and photon counting distributions (PCDs) of monomeric EGFP (A) and *cgre*GFP (B). PCDs were calculated with bin times of 50 (●) and 100 μs (○). The experimental intensity fluctuations are shown at the top. For EGFP 2.4 × 10^5 photons and for *cgre*GFP 6.5 × 10^5 photons were collected. Residuals are plotted below each curve. PCH analysis was performed with a polynomial profile. Recovered parameters are listed in Table 3. Global criterion values are as follows: χ^2 = 1.35 for EGFP, and χ^2 = 1.17 for *cgre*GFP.

averaged. As described in Materials and Methods, from a single fluorescence fluctuation trace, the autocorrelation function (ACF) and the photon counting distribution (PCD) can be calculated. The simplest model function, $G_{\text{theor}}(t)$, to fit the experimental ACF, $G_{\text{exp}}(t)$, of a single molecular species has the following form:

$$G_{\text{theor}}(t) = 1 + \frac{1}{N_{\text{eff}}} \times \frac{1 - F_{\text{trip}} + F_{\text{trip}} \exp(-t/\tau_{\text{trip}})}{1 - F_{\text{trip}}} \times \frac{1}{1 + \frac{t}{\tau_{\text{dif}}}\sqrt{1 + \frac{t}{a^2 \tau_{\text{dif}}}}} \quad (7)$$

where N_{eff} is the number of molecules in a three-dimensional Gaussian-shaped observation volume (V_{eff}), F_{trip} and τ_{trip} are the fraction and relaxation time of molecules in the triplet state, respectively, a is the structure parameter ($a = \omega_z/\omega_{xy}$, where ω_z and ω_{xy} are the axial and equatorial radii, respectively, of the confocal detection volume), and τ_{dif} is the lateral diffusion time (the time that the molecule spends in the confocal volume), which is related to the diffusion coefficient D_t via the relationship $\tau_{\text{dif}} = \omega_{xy}^2/(4D_t)$. The observation volume can be approximated by the relationship $V_{\text{eff}} = \pi^{3/2}\omega_{xy}^2\omega_z^2$. Analysis of the experimental ACF, $G_{\text{exp}}(t)$, using eq 7 yields the following parameters: τ_{dif}, F_{trip}, τ_{trip}, N_{eff}, and a. From N_{eff} and V_{eff}, we can obtain the protein concentrations. PCH analysis yields the molecular brightness (q_0) and number of molecules (N_{eff}) but, depending on the bin time, should also be corrected for dynamic processes such as those modeled in FCS. Therefore, the model functions of ACF and PCH contain a number of common parameters, which can be linked in global analysis. For more details, see refs 23 and 24.

Examples of fluorescence fluctuation experiments and associated analysis of EGFP and *cgre*GFP in aqueous buffer are given in Figure 7. All parameters are listed in Table 3. There are two pieces of evidence that *cgre*GFP is a dimeric protein. First, the translational diffusion constant D_t of *cgre*GFP (55.1 $\mu m^2\ s^{-1}$) is distinctly slower than that of (monomeric) EGFP (82.7 $\mu m^2\ s^{-1}$) and comparable to that of "synthetic" dimeric EGFP (54.3 $\mu m^2\ s^{-1}$) recently published.[24] Second, the brightness value q_0 of *cgre*GFP is a factor of 1.7 higher than that of EGFP. For a pure dimer, one would expect a difference of a factor of 2, but one should keep in mind that energy loss is taking place via radiationless energy exchange between the chromophores (homo-FRET). Moreover, the chromophoric group in EGFP is not in the same molecular environment as that in *cgre*GFP. It is further noteworthy that at 2.6 nM *cgre*GFP is still dimeric. The observation that the lifetime of the triplet state is much longer in the case of *cgre*GFP (11.6 μs) as compared to that of EGFP (3.0 μs) is quite remarkable. After analysis of the ACF of aromatic dye molecules (such as rhodamines) in air-equilibrated, aqueous solutions, triplet lifetimes in the range of 1−4 μs, like in EGFP, are always recovered.[35] When a molecule enters the triplet state via intersystem crossing, the molecule appears to be dark, as no fluorescent photons are emitted. When the molecule returns to the ground state, another photocycle can occur, explaining why the triplet state is a source of fluorescence fluctuations. The 12 μs relaxation time, however, is too long for a triplet-state lifetime. We therefore suggest that this relaxation is due to blinking behavior of *cgre*GFP creating long-lived dark states (blinking and switching effects in single visible-fluorescent proteins are reviewed in ref 36). As mentioned above for the ensemble-type single-photon timing measurements, there is a finite probability that two chromophores in the same protein are simultaneously excited and will not exchange energy. In a confocal microscope, the laser excitation density is quite large and the chance that the fluorescence burst arises from two excited molecules is

Table 3. Global Analysis of the Autocorrelation Function and Photon Counting Distributions of EGFP and *cgre*GFP at 20 °C

protein	F_{trip} (−)	τ_{trip} (μs)	τ_{dif} (μs)	D_t ($\mu m^2\ s^{-1}$)	N_{eff} (−)	[protein] (nM)	q_0 (cpmps)[a]
EGFP	0.18 ± 0.02	3.0 ± 0.5	62.4 ± 0.5	82.7 ± 0.1	1.61	8.0	34480
*cgre*GFP	0.19 ± 0.01	11.6 ± 0.1	93.7 ± 0.1	55.1 ± 0.1	0.52	2.6	57750

[a] Units of the number of photon counts emitted per molecule per second.

appreciable. Two chromophores in the triplet state may lead to a dark state, which might last longer than the triplet state of a single chromophore. Once the triplet state has been reached, the possible involvement of radical chemistry in phototransformation as recently proposed[37,38] deserves further investigation.

DISCUSSION

A major topic addressed in this work is the ability of GFP to shift the photoprotein bioluminescence color at micromolar concentrations of the proteins where donor−acceptor separations far exceed the Förster distance, unless they are constrained within a tight protein−protein complex. A spatial structure of a clytin−*cgre*GFP complex has been published,[10] but the affinity is very weak, in the millimolar range. These results similarly show no detectable interaction of *cgre*GFP with Ca^{2+}-discharged clytin, the final product of the bioluminescence reaction. We propose that, in the course of the bioluminescence pathway, a more tightly binding complex of a distinct calcium-bound clytin intermediate with the *cgre*GFP must be formed. We draw attention to the fact that the bioluminescence donor is not the excited state of the Ca^{2+}-discharged clytin (λ_{max} = 506 nm) but the S_1 state responsible for the blue bioluminescence spectrum (λ_{max} = 470 nm).[10,12] It has been shown that mutations that make small changes in the environment of the protein-bound coelenteramide anion lead to shifts in both the bioluminescence and Ca^{2+}-discharged photoprotein fluorescence within the range of 453−509 nm.[39] Therefore, it is suggested that, following the emission of bioluminescence, there is a shift from the calcium−clytin conformation that presents a tight binding site to *cgre*GFP to one allowing *cgre*GFP to be released.

This idea of a transient complex can draw support from the striking similarity between its properties and those of the bacterial bioluminescence system. The bacterial luciferase before reaction associates only weakly ($K_d \sim 1$ mM) with lumazine protein, its conjugate antenna protein unrelated to GFP,[40] yet bacterial bioluminescence spectra are modulated upon addition of lumazine protein also at concentrations in the micromolar region. This system is well suited for investigation by polarized dynamic fluorescence, and thereby, the occurrence of a bacterial luciferase reaction intermediate−lumazine protein complex was shown.[15,16,41,42] Recently, on the basis of the crystal structures, a computational model of the luciferase−lumazine protein complex has been constructed.[43] It reveals a donor−acceptor separation of <20 Å.

At present, no information about Ca^{2+}-regulated photoprotein intermediates is available. However, we can make an estimate of interaction parameters first by calculating the bimolecular (or encounter) rate constant k_e for a diffusion-controlled reaction between clytin and *cgre*GFP:[44]

$$k_e = 4\pi r_0 (D_C + D_G) \times 10^{-3} \times N_0 \qquad (8)$$

where D_C and D_G are the clytin and *cgre*GFP diffusion constants (87×10^{-8} and 55.1×10^{-8} $cm^2\ s^{-1}$, respectively; note that 1×10^{-8} $cm^2\ s^{-1} = 1\ \mu m^2\ s^{-1}$), r_0 is the distance of closest approach or the sum of the radii (6×10^{-7} cm), and N_0 is Avogadro's number. The diffusion constant of clytin ($D_C = 87 \times 10^{-8}$ $cm^2\ s^{-1}$) can be easily calculated from the diffusion constant of EGFP, D_E (Table 3), and the rotational correlation times of clytin (ϕ_C = 12 ns) and EGFP (ϕ_E = 14 ns).

$$\frac{D_C}{D_E} = \left(\frac{\phi_E}{\phi_C}\right)^{1/3} \qquad (9)$$

Assuming that the radius of clytin is 20 Å[12] and that of the *cgre*GFP dimer is 40 Å (Figure 5), we find $r_0 = 6.0 \times 10^{-7}$ cm and eq 8 gives a k_e of 6.4×10^9 $M^{-1}\ s^{-1}$.

Equation 8 provides only the theoretical limit for the rate constant for the encounter of the two proteins. However, not every encounter needs to yield a productive complex, e.g., one with the required stereospecificity. Following transition-state theory and experimental evidence collated in ref 45, the majority of values of productive protein−protein association rate constants that we will label k_a lie in the range of 10^6 to 4×10^8 $M^{-1}\ s^{-1}$, although some approach the diffusion-limited encounter rate constant of 6.4×10^9 $M^{-1}\ s^{-1}$ obtained via eq 8.

Addition of Ca^{2+} to clytin (phialidin) triggers light emission rising in the time range of 1−10 ms.[7] This reflects the rate-limiting step in the bioluminescence reaction pathway and, presumably, the lifetime of the critical intermediate calcium-bound clytin, conjectured here to have a high affinity for *cgre*GFP. Assuming maximal values ($k_d = 10^3\ s^{-1}$, and $k_a = 10^9\ M^{-1}\ s^{-1}$), the calcium-bound clytin−*cgre*GFP affinity would lie in the micromolar range. In a recent report, a complete shift in the bioluminescence spectrum of clytin was observed when 2.5 μM clytin was mixed with 2.5 μM *cgre*GFP.[12] Thus, the feasibility of a micromolar affinity of the intermediate complex would account for the bioluminescence spectral shift occurring at micromolar levels. To support this proposal, the rate constants k_d and k_a must be experimentally determined, for instance, by rapid-scanning stopped-flow experiments.

In this work, we show that the final product Ca^{2+}-discharged clytin has no measurable interaction with *cgre*GFP. If we assume its affinity is similar to that of clytin itself ($K_d \approx 1$ mM), then such a weak affinity of the final product would result, after FRET in the intermediate complex, in the "relaxed" proteins being quickly released from each other and made available for a subsequent round.

Why do we not observe even a weak protein−protein interaction here with time-resolved fluorescence anisotropy? The answer to this question is largely technical. Besides the ability to stabilize the bacterial luciferase intermediate for up to 24 h, the bound lumazine chromophore has a rather long fluorescence lifetime of 14 ns,[40] which is 5 times longer than that of *cgre*GFP. This makes the time span of measuring anisotropy around 60 ns, which is much longer than the corresponding time span of 18 ns for *cgre*GFP (see Figure 4). In addition, the lumazine protein has a mass of 20 kDa, and luciferase has a mass of 80 kDa, giving the fluorescent complex an overall mass of 100 kDa, which is easily distinguishable in the anisotropy decay. In the *C. gregaria* bioluminescent system, the corresponding antenna protein *cgre*GFP is larger than the photoprotein donor and the mass change is much smaller.

dx.doi.org/10.1021/bi101671p |*Biochemistry* 2011, 50, 4232–4241

Another question is why the *cgre*GFP antenna protein is dimeric. Intuitively, it can be argued that the range for interaction with clytin becomes larger because the Förster distance increases. The excited coelenteramide produced from the Ca^{2+}-triggered clytin "sees" two acceptor molecules in the dimeric antenna protein. This makes the effective extinction coefficient of the acceptor a factor of 2 larger, increasing the overlap integral and consequently the Förster distance. Resonance energy transfer to the acceptor will efficiently occur over larger distances. From the dimensions of the *cgre*GFP protein chains and with the donor and acceptor ligands lying more or less in their centers, their physical separation could not be <25 Å (Figure 5). At the total protein concentration of 5 μM mentioned above, the FRET efficiency is almost 100%,[12] meaning that, aided by an optimal orientation of transition moment dipoles, R_0 must be substantially greater than this 25 Å physical separation.

Can we make an extrapolation to the bioluminescence from the animal from the reaction in the photocytes? The interior of the jellyfish photocytes is crowded with macromolecules, including the photoproteins and antenna proteins estimated in *Aequorea* at concentrations up to 1 mM each.[13,46] Crowding has large effects on rates and equilibria of protein−protein interactions.[47] The excluded volume that is associated with crowding lowers the rate of translational diffusion of tracer proteins in concentrated protein solutions.[48] The viscosity of the cytoplasm is highly exemplified by the slower translational diffusion of GFP (D_t = 24 $\mu m^2\ s^{-1}$) in, for instance, vegetative *Dictyostelium* cells immobilized in 3% agarose.[22] Rotational and translational motions of proteins in crowded solutions experience different microviscosities. It has been shown that the diffusion constants depend not only on the microviscosity but also on the size ratio of the tracer protein and macromolecular cosolute,[49] which are effectively the same in photocytes. Now we can estimate the apparent translational diffusion constants in the cytoplasm, assuming that the cytoplasmic viscosity is 3 times that of water, to be half of the those in aqueous solution: for clytin, $D_C = 43.5 \times 10^{-8}\ cm^2\ s^{-1}$, and for *cgre*GFP, $D_G = 27.5 \times 10^{-8}\ cm^2\ s^{-1}$. The diffusion-controlled encounter rate constant (eq 8) is half of that in water ($k_e = 3.2 \times 10^9\ M^{-1}\ s^{-1}$). For the reported clytin−*cgre*GFP equilibrium dissociation constant of ≈1 mM, both proteins would be already present in a preformed weak complex.[10] As discussed in ref 49, rotational motion can also contribute to transport, as a 180° rotation is equivalent to the spatial displacement in the order of a protein diameter. Rotations may assist in specific molecular recognition.

The in vivo bioluminescence spectra of several animals or from their tissue samples reveal nearly exact correspondence to the fluorescence of GFP, implying near 100% bioluminescence FRET efficiency.[5,6,50] We propose that in the photocyte the photoprotein and GFP are poised in a weak complex that, upon the appearance of the Ca^{2+} trigger, is constrained to optimize the bioluminescence FRET process and become a 100% efficient green photon factory.

AUTHOR INFORMATION

Corresponding Author

*E-mail: jlee@uga.edu. Phone: (706) 549-4630. Fax: (706) 542-1738.

Funding Sources

This work was supported by NATO Collaborative Linkage Grant 979229, Grants SB RAS No. 2 and RFBR 08-04-92209, 09-04-12022, and 09-04-00172, the MCB program of the Russian Academy of Sciences, and Bayer AG.

ABBREVIATIONS

ACF, autocorrelation function; ECFP, cyan-fluorescent protein, enhanced; ESPT, excited-state proton transfer; FCS, fluorescence correlation spectroscopy; FFS, fluorescence fluctuation spectroscopy; FRET, Förster resonance energy transfer; *cg*GFP, natural GFP from *C. gregaria*; *cgre*GFP, recombinant *cg*GFP; *av*GFP, natural GFP from *A. victoria*; *avre*GFP, recombinant *av*GFP; EGFP, enhanced GFP; PCD, photon counting distribution; PCH, photon counting histogram; TCSPC, time-correlated single-photon counting; YFP, yellow-fluorescent protein.

REFERENCES

(1) Shimomura, O. (1998) The discovery of green-fluorescent protein. In *Green-Fluorescent Protein* (Chalfie, M., and Kain, S., Eds.) pp 3−15, Wiley-Liss, New York.

(2) Matz, M. V., Fradkov, A. F., Labas, Y. A., Savitsky, A. P., Zaraisky, A. G., Markelov, M. L., and Lukyanov, S. A. (1999) Fluorescent proteins from nonbioluminescent *Anthozoa* species. *Nat. Biotechnol. 17*, 969–973.

(3) Ward, W. W. (1998) Biochemical and physical properties of green-fluorescent protein. In *Green-Fluorescent Protein* (Chalfie, M., and Kain, S., Eds.) pp 45−75, Wiley-Liss, New York.

(4) Shimomura, O. (2006) *Bioluminescence: Chemical Principles and Methods*, World Scientific Publishing, Singapore.

(5) Morin, J. G., and Hastings, J. W. (1971) Energy transfer in a bioluminescent system. *J. Cell. Physiol. 77*, 313–318.

(6) Wampler, J. E., Hori, K., Lee, J. W., and Cormier, M. J. (1971) Structured bioluminescence. Two emitters during both the *in vitro* and the *in vivo* bioluminescence of the sea pansy. *Biochemistry 10*, 2903–2909.

(7) Levine, L. D., and Ward, W. W. (1982) Isolation and characterization of a photoprotein, "phialidin", and a spectrally unique green-fluorescent protein from the bioluminescent jellyfish *Phialidium gregarium*. *Comp. Biochem. Physiol. 72B*, 77–85.

(8) Vysotski, E. S., and Lee, J. (2004) Ca^{2+}-regulated photoproteins: Structural insight into the bioluminescence mechanism. *Acc. Chem. Res. 37*, 405–415.

(9) Haddock, S. H. D., Moline, M. A., and Case, J. F. (2010) Bioluminescence in the sea. *Annu. Rev. Mar. Sci. 2*, 443–493.

(10) Titushin, M. S., Feng, Y., Stepanyuk, G. A., Li, Y., Markova, S. V., Golz, S., Wang, B. C., Lee, J., Wang, J., Vysotski, E. S., and Liu, Z. J. (2010) NMR-derived topology of a GFP-photoprotein energy transfer complex. *J. Biol. Chem. 285*, 40891–40900.

(11) Ward, W. W., and Cormier, M. J. (1978) Energy transfer via protein-protein interaction in *Renilla* bioluminescence. *Photochem. Photobiol. 27*, 389–396.

(12) Markova, S. V., Burakova, L. P., Frank, L. A., Golz, S., Korostileva, K. A., and Vysotski, E. S. (2010) Green-fluorescent protein from the bioluminescent jellyfish *Clytia gregaria*: cDNA cloning, expression, and characterization of novel recombinant protein. *Photochem. Photobiol. Sci. 9*, 757–765.

(13) Morise, H., Shimomura, O., Johnson, F. H., and Winant, J. (1974) Intermolecular energy transfer in the bioluminescent system of *Aequorea*. *Biochemistry 13*, 2656–2662.

(14) Prasher, D. C., Eckenrode, V. K., Ward, W. W., Prendergast, F. G., and Cormier, M. J. (1992) Primary structure of the *Aequorea victoria* green-fluorescent protein. *Gene 111*, 229–233.

(15) Petushkov, V. N., Gibson, B. G., and Lee, J. (1995) Properties of recombinant fluorescent proteins from *Photobacterium leiognathi* and their interaction with luciferase intermediates. *Biochemistry 34*, 3300–3309.

(16) Petushkov, V. N., Gibson, B. G., and Lee, J. (1996) Direct measurement of excitation transfer in the protein complex of bacterial luciferase hydroxyflavin and the associated yellow fluorescence proteins from *Vibrio fischeri Y1*. *Biochemistry 35*, 8413–8418.

(17) Illarionov, B. A., Frank, L. A., Illarionova, V. A., Bondar, V. S., Vysotski, E. S., and Blinks, J. R. (2000) Recombinant obelin: Cloning

and expression of cDNA, purification and characterization as a calcium indicator. *Methods Enzymol. 305*, 223–249.

(18) Vysotski, E. S., Liu, Z. J., Rose, J., Wang, B. C., and Lee, J. (2001) Preparation and X-ray crystallographic analysis of recombinant obelin crystals diffracting to beyond 1.1 Å. *Acta Crystallogr. D57*, 1919–1921.

(19) Gasparian, M. E., Ostapchenko, V. G., Schulga, A. A., Dolgikh, D. A., and Kirpichnikov, M. P. (2003) Expression, purification, and characterization of human enteropeptidase catalytic subunit in *Escherichia coli*. *Protein Expression Purif. 31*, 133–139.

(20) Borst, J. W., Hink, M. A., van Hoek, A., and Visser, A. J. (2005) Effects of refractive index and viscosity on fluorescence and anisotropy decays of enhanced cyan and yellow fluorescent proteins. *J. Fluoresc. 15*, 153–160.

(21) Borst, J. W., Laptenok, S. P., Westphal, A. H., Kühnemuth, R., Hornen, H., Visser, N. V., Kalinin, S., Aker, J., van Hoek, A., Seidel, C. A., and Visser, A. J. (2008) Structural changes of yellow Cameleon domains observed by quantitative FRET analysis and polarized fluorescence correlation spectroscopy. *Biophys. J. 95*, 5399–5411.

(22) Ruchira, Hink, M. A., Bosgraaf, L., van Haastert, P. J., and Visser, A. J. (2004) Pleckstrin homology domain diffusion in *Dictyostelium* cytoplasm studied using fluorescence correlation spectroscopy. *J. Biol. Chem. 279*, 10013–10019.

(23) Hink, M. A., Shah, K., Russinova, E., de Vries, S. C., and Visser, A. J. (2008) Fluorescence fluctuation analysis of *Arabidopsis thaliana* somatic embryogenesis receptor-like kinase and brassinosteroid insensitive 1 receptor oligomerization. *Biophys. J. 94*, 1052–1062.

(24) Skakun, V. V., Engel, R., Digris, A. V., Borst, J. W., and Visser, A. J. (2011) Global analysis of autocorrelation functions and photon counting distributions. *Front. Biosci. (Elite Ed.) 3*, 489–505.

(25) Müller, C. B., Loman, A., Pacheco, V., Koberling, F., Willbold, D., Richtering, W., and Enderlein, J. (2008) Precise measurement of diffusion by multi-color dual-focus fluorescence correlation spectroscopy. *Eur. Phys. Lett. 83*, 46001.

(26) van Oort, B., Eremeeva, E. V., Koehorst, R. B., Laptenok, S. P., van Amerongen, H., van Berkel, W. J., Malikova, N. P., Markova, S. V., Vysotski, E. S., Visser, A. J., and Lee, J. (2009) Picosecond fluorescence relaxation spectroscopy of the calcium-discharged photoproteins aequorin and obelin. *Biochemistry 48*, 10486–10491.

(27) Uskova, M. A., Borst, J. W., Hink, M. A., van Hoek, A., Schots, A., Klyachko, N. L., and Visser, A. J. (2000) Fluorescence dynamics of green-fluorescent protein in AOT reversed micelles. *Biophys. Chem. 87*, 73–84.

(28) Cotlet, M., Hofkens, J., Maus, M., Gensch, T., Van der Auweraer, M., Michiels, J., Dirix, G., Van Guyse, M., Vanderleyden, J., Visser, A. J., and De Schryver, F. C. (2001) Excited-state dynamics in the enhanced green fluorescent protein mutant probed by picosecond time-resolved single photon counting spectroscopy. *J. Phys. Chem. B 105*, 4999–5006.

(29) Patterson, G. H., and Lippincott-Schwartz, J. (2002) A photoactivatable GFP for selective photolabeling of proteins and cells. *Science 297*, 1873–1877.

(30) Bastiaens, P. I., van Hoek, A., Benen, J. A., Brochon, J. C., and Visser, A. J. (1992) Conformational dynamics and intersubunit energy transfer in wild-type and mutant lipoamide dehydrogenase from *Azotobacter vinelandii*. A multidimensional time-resolved polarized fluorescence study. *Biophys. J. 63*, 839–853.

(31) Rosell, F. I., and Boxer, S. G. (2003) Polarized absorption spectra of green-fluorescent protein single crystals: Transition dipole moment directions. *Biochemistry 42*, 177–183.

(32) McMeekin, T. L., Wilensky, M., and Groves, M. L. (1962) Refractive indices of proteins in relation to amino acid composition and specific volume. *Biochem. Biophys. Res. Commun. 7*, 151–156.

(33) Knox, R. S., and van Amerongen, H. (2002) Refractive index dependence of the Förster resonance excitation transfer rate. *J. Phys. Chem. B 106*, 5289–5293.

(34) Toptygin, D., Savtchenko, R. S., Meadow, N. D., Roseman, S., and Brand, L. (2002) Effect of the solvent refractive index on the excited-state lifetime of a single tryptophan residue in a protein. *J. Phys. Chem. B 106*, 3724–3734.

(35) Widengren, J., Mets, U., and Rigler, R. (1995) Fluorescence correlation spectroscopy of triplet states in solution: A theoretical and experimental study. *J. Phys. Chem. 99*, 13368–13379.

(36) Moerner, W. E. (2002) Single-molecule optical spectroscopy of autofluorescent proteins. *J. Chem. Phys. 117*, 10925–10937.

(37) Bogdanov, A. M., Dmitriy, M., Chudakov, D. M., Mishin, A. S., Yampolsky, I. V., Subach, F. V., Verkhusha, V. V., Belousov, V. V., Lukyanov, S., and Lukyanov, K. A. (2009) Green-fluorescent proteins are light-induced electron donors. *Nat. Chem. Biol. 5*, 459–461.

(38) Adam, V., Carpentier, P., Violot, S., Lelimousin, M., Darnault, C., Nienhaus, G. U., and Bourgeois, D. (2009) Structural basis of X-ray-induced transient photobleaching in a photoactivatable green fluorescent protein. *J. Am. Chem. Soc. 131*, 18063–18065.

(39) Stepanyuk, G. A., Golz, S., Markova, S. V., Frank, L. A., Lee, J., and Vysotski, E. S. (2005) Interchange of aequorin and obelin bioluminescence color is determined by substitution of one active site residue of each photoprotein. *FEBS Lett. 579*, 1008–1014.

(40) Visser, A. J., and Lee, J. (1982) Association between lumazine protein and bacterial luciferase: Direct demonstration from the decay of the lumazine emission anisotropy. *Biochemistry 21*, 2218–2226.

(41) Lee, J., O'Kane, D. J., and Gibson, B. G. (1989) Bioluminescence spectral and fluorescence dynamics study of the interaction of lumazine protein with the intermediates of bacterial luciferase bioluminescence. *Biochemistry 28*, 4263–4271.

(42) Petushkov, V. N., Ketelaars, M., Gibson, B. G., and Lee, J. (1996) Interaction of *Photobacterium leiognathi* and *Vibrio fischeri Y1* luciferases with fluorescent (antenna) proteins: Bioluminescence effects of the aliphatic additive. *Biochemistry 35*, 12086–12093.

(43) Sato, Y., Shimizu, S., Ohtaki, A., Noguchi, K., Miyatake, H., Dohmae, N., Sasaki, S., Odaka, M., and Yohda, M. (2010) Crystal structures of the lumazine protein from *Photobacterium kishitanii* in complexes with the authentic chromophore, 6,7-dimethyl- 8-(1′-D-ribityl) lumazine, and its analogues, riboflavin and flavin mononucleotide, at high resolution. *J. Bacteriol. 192*, 127–133.

(44) Cantor, C. R., and Schimmel, P. R. (1980) *Biophysical Chemistry*, Chapter 16, W. H. Freeman, San Francisco.

(45) Alsallaq, R., and Zhou, H. X. (2007) Prediction of protein-protein association rates from a transition-state theory. *Structure 15*, 215–224.

(46) Cutler, M. W. (1995) Characterization and energy transfer mechanism of the green-fluorescent protein from *Aequorea victoria*. Ph. D. Thesis, Rutgers University, New Brunswick, NJ.

(47) Ellis, R. J. (2001) Macromolecular crowding: Obvious but underappreciated. *Trends Biochem. Sci. 26*, 597–604.

(48) Muramatsu, N., and Minton, A. P. (1988) Tracer diffusion of globular proteins in concentrated protein solutions. *Proc. Natl. Acad. Sci. U.S.A. 85*, 2984–2988.

(49) Lavalette, D., Hink, M. A., Tourbez, M., Tetreau, C., and Visser, A. J. (2006) Proteins as micro viscosimeters: Brownian motion revisited. *Eur. Biophys. J. 35*, 517–522.

(50) Wampler, J. E., Karkhanis, Y. D., Morin, J. G., and Cormier, M. J. (1973) Similarities in the bioluminescence from the *Pennatulacea*. *Biochim. Biophys. Acta 314*, 104–109.